GEOLOGICA BALCANICA 51 (2), Sofia, August 2022, pp. 27–35.

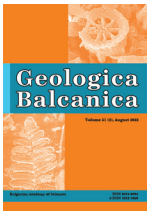

REY in pore waters of sediments hosting Fe-Mn nodules of the Interoceanmetal exploration area in the Clarion-Clipperton Fracture Zone, NE Pacific

Zlatka Milakovska[1], Atanas Hikov[1], Valcana Stoyanova[2], Irena Peytcheva[1], Valentina Lyubomirova[3], Tomasz Abramowski[2, 4]

[1] Geological Institute, Bulgarian Academy of Sciences, Acad. G. Bonchev Str., Bl. 24, 1113 Sofia, Bulgaria; e-mails: zlatkam@geology.bas.bg; ahikov@geology.bas.bg; irena.peytcheva@erdw.ethz.ch
[2] Interoceanmetal Joint Organization, 9 Cyryla i Metodego Str., 71-541 Szczecin, Poland; e-mail: valcana.stoyanova@iom.gov.pl
[3] Faculty of Chemistry and Pharmacy, Sofia University "St Kliment Ohridski", 1 James Bourchier Blvd, 1164 Sofia, Bulgaria; e-mails: vlah@chem.uni-sofia.bg
[4] Maritime University of Szczecin, 1/2 Wały Chrobrego, 70-500 Szczecin, Poland; e-mail: t.abramowski@am.szczecin.pl

(Received: 28 June 2022; accepted in revised form: 27 July 2022)

Abstract. Our study is focused on REE and yttrium (REY) geochemistry of pore waters from core-box sediments. The samples were collected from the 0–5 cm, 10–15 cm, 25–30 cm, and 35–40 cm depth intervals of four stations of the eastern part of block H_22 of IOM license area of the Clarion-Clipperton Fracture Zone, NE Pacific. The REE studies in marine pore fluids were limited by analytical challenges. The pore water analysis we applied is based on a modern, improved analytical technique (ICP-MS, Perkin-Elmer SCIEX Elan DRC-e) with a cross-flow nebulizer and a spectrometer optimized (RF, gas flow, lens voltage) using a quadrupole cell in a DRC (Dynamic Reaction Cell) mode that allowed us to define the whole suite of REE. The ΣREY values of the samples vary from 4.05 µg/l to 106.34 µg/l. The REE content is at least one order of magnitude higher than the oceanic water. We followed the natural variations of La, Lu, Ce, and Y in absolute concentrations for station 3607. Cerium and Y are slightly enriched around the water-sediment interface, while La and Lu are enriched in the deeper layers. PAAS normalized REY patterns show a pronounced negative Ce/Ce* ratio together with a little MREE and HREY enrichment. The relatively "flat" REE patterns are typical for the shallow open ocean and characterize REE released from the organic matter degradation. We assume that the decomposition of and adsorption on organic matter and oxidation conditions are the main factors for REE fractionation in the pore water. The reason for some scatter in our REY data might be linked to bioturbation that has affected the sediment profiles.

Milakovska, Z., Hikov, A., Stoyanova, V., Peytcheva, I., Lyubomirova, V., Abramowski, T. 2022. REY in pore waters of sediments hosting Fe-Mn nodules of the Interoceanmetal exploration area in the Clarion-Clipperton Fracture Zone, NE Pacific. *Geologica Balcanica* 51 (2), 27–35.

Keywords: rare earth elements, yttrium, pore waters, metalliferous sediments, polymetallic nodules, Clarion-Clipperton Fracture Zone.

INTRODUCTION

Fe-Mn polymetallic nodules and sediments are potential source of critical elements, especially of Rear Earth Elements and yttrium (REY) (*e.g.*, Kato, 2011; Hein *et al.*, 2013; Baláž, 2021). Still, there are gaps in our understanding of the element sources and the diversity of genetic processes (sorption, scavenging, ion-exchange, etc.), complicated by the organic-geochemical and bioturbation processes. The deep-sea sediments hosting Fe-Mn nodules are soaked in pore waters considered an

https://doi.org/10.52321/GeolBalc.51.2.27

important source of trace metals, so in the present study we focus on the REY geochemistry of the pore waters. Our aim was to reveal their applicability to genetic interpretations and assessment of the potential as a REY source. The research is in accordance with ISBA/19/LTC/8 recommendations for chemical oceanography to "collect information on background water column chemistry, including water overlying the resource, in particular on metals and other elements that may be released during the mining process."

The marine geochemistry of REE has attracted increasing attention as they serve as: (1) a useful probe in understanding scavenging processes of particulate matter (Elderfield and Greaves, 1982; Byrne and Kim, 1990); (2) natural analog of actinides and transuranics, such as Ac, Th, Pu, Am, Cm and Cf in the marine environment (Bowen *et al*., 1980; Livingston and Anderson, 1983); and (3) tracers of water masses and ocean circulation (Zhang and Nozaki, 1996). The REE studies in marine pore fluids were limited by analytical challenges (Kim *et al*., 2012), and too few pore water data are available from the stations to make statements about the concentration trend with depth.

In our case study, we focus on REY geochemical characteristics and distribution in the ocean pore waters of the deep-sea sediments of four stations (3607, 3609-1, 3615 and 3629) from the Interoceanmetal (IOM) exploration area (Fig. 1) in the Clarion-Clipperton Fracture Zone (CCZ). The samples were collected during the IOM-2019 research cruise. For data acquisition, we applied a modern, improved analytical technique (ICP-MS, Perkin-Elmer SCIEX Elan DRC-e) with a cross-flow nebulizer and a spectrometer optimized (RF, gas flow, lens voltage) using a quadrupole cell in a DRC (Dynamic Reaction Cell) mode (Lyubomirova *et al.*, 2020a). It allowed us to define the whole suite of REE in depth profiles, whereas subsequently the REY distributions were Post Archean Australian Shale (PAAS) normalized and conclusions were made about the elements anomalies and sourcing.

GEOLOGICAL SETTING

The IOM license area is situated in the eastern part of the Clarion-Clipperton Fracture Zone, NE Pacific, which is considered most perspective for nodule exploitation. It is designated as the H22_NE exploitable block and covers an area of 630 km^2 of the seafloor between 11°06′–11°26′N latitude and 119°25′–119°42′W longitude at depth varying from 4,300 m to 4,500 m (Fig. 1). The analyzed four stations 3607, 3609-1, 3615 and 3629 are distributed among various geomorphological types, represent-

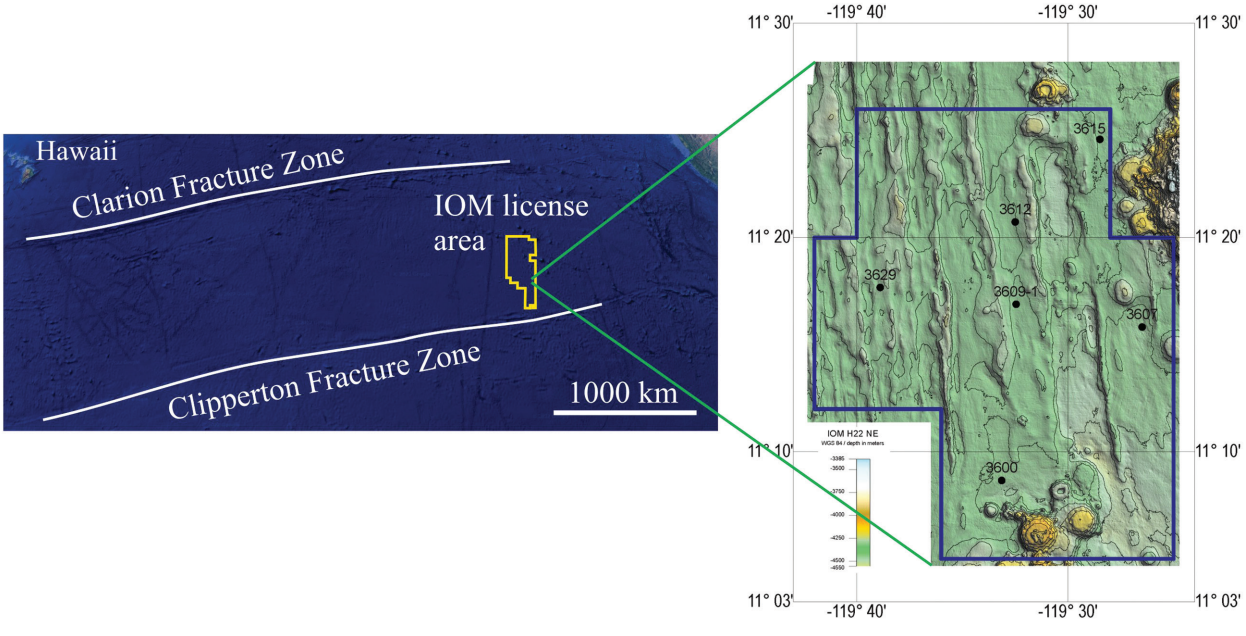

Fig. 1. Geomorphological map of the seafloor with location of the sampling area in the IOM exploration site in the eastern part of the Clarion-Clipperton Fracture Zone, NE Pacific (the background is a satellite image provided by Google Earth).

ed mostly by undulating hilly plains intersected by longitudinal ridges oriented in a meridional direction, and a sub-parallel volcanic massif. All stations sampled are located below the critical carbonate compensation depth (CCD). The sedimentary cover within the IOM exploration area is about 100 m thick. The sediment profile is topped by siliceous silty clay. Sediments of this layer contain 3.04–28.6% of amorphous silica and are characterized by a reduced bulk density and an increased moisture content (Baláž, 2021; Skowronek *et al*., 2021).

At all stations, the dominating sediment type is light brown siliceous silty clay with irregular dark patches along the entire core down to 45 cm in depth. The top layer of thickness 7–12 cm comprises a semiliquid, predominantly dark brown, siliceous silty clay, denoted as geochemically active layer (GAL). The GAL is the medium for polymetallic nodule formation. The redox potential (Eh) values for the GAL range from +462 mV to +545 mV, average +494 mV, and show a tendency to decrease with depth. Maximum redox potential value (+547 mV) was obtained for slightly siliceous silty clay at station 3615 at a depth of 30 cm. The sediments at this station are dark and contain abundant radiolarian skeletons, sponge spicules, micronodules, and clay aggregates. The active reaction (pH) of the deep-sea environment for all sediments is mostly neutral, varying from 7.01 to 7.52, averaging 7.36 (Milakovska *et al*., 2021).

Previous results of Milakovska *et al*. (in preparation) for the sediments in the area indicated fine silt predomination. The sediments are poorly sorted, with bimodal particle size distribution. The silt (50–84%) and sandy (9–31%) fractions show opposite trends of distribution, and the clay fraction quantity increases with depth. The mineral composition according to bulk XRD data is uniform in quality and quantity. An amorphous phase (84–88%) predominates and represents biogenic opal, authigenic Fe-Mn (hydro)oxides and clay minerals. These grain size and phase compositions define the sediments as clayey siliceous oozes. The crystalline phases of illite, kaolinite, chlorite, quartz, and andesine represent a detrital component, while halite, cristobalite, and barite are of authigenic origin. Illite, illite/smectite, chlorite/vermiculite and kaolinite, and quartz admixture were detected in all fractions <2 μm (Milakovska *et al*., 2021).

The chemical composition of the sediment samples is similar in the four stations and some small differences are related to the station location and depth interval sampled. The values for Si, Al, Fe, K, Mg and Ti show low variations among the layers and slightly increase with depth. Manganese content varies from 0.16% to 0.70%, being highest for the top 7–12 cm and decreases with depth. The Mn/Fe ratio, Co, Ni, Cu and Ba have the highest values in the upper layer, and lowest in the deepest levels. The highest Mn, Co and Cu concentrations are defined for station 3615, while the highest Ba and P values are found for stations 3629 and 3615. The ΣREE values in the sediments vary from 196 to 358 ppm, and the ΣREY – between 247 and 458 ppm. The stations 3629 and 3615 have the highest REE and Y content without any significant variations between the layers. PAAS-normalized REE patterns have MREE and HREE enrichment. All samples show strong negative Ce ($Ce/Ce^* = 0.70$) anomaly, positive Eu ($Eu/Eu^* = 1.19$) anomaly, and weak positive Y ($Y/Y^* = 1.03$) anomaly (Hikov *et al*., 2022).

SAMPLING STRATEGY AND METHODS OF STUDY

Sampling strategy

The core-box sediments were collected from the intervals 0–5 cm, 10–15 cm, 25–30 cm and 35–40 cm from stations of block H_22 of IOM (Fig. 1). The sediment samples for pore water extraction were selected on-board and the individual depth intervals followed the recommendations of the International Seabed Authority ISBA/19/LTC/8 to collect information on metals and other elements of the background water column in the region of resource exploration. The water sampling was done using centrifuging by 11000 rpm. The extractions of *ca*. 300 ml of pore water were filtrated through a membrane filter (Vladipore, type MFAC-OC-2, pore diameter of 0.45 μm) using a laboratory vacuum pump with polycarbonate filter (Sartorius stedium 16510). The filtered water samples were stored in plastic bottles of 150 ml in volume and stabilized by concentrated nitric acid of 0.15 ml.

ICP-MS analyses of the pore waters

The chemical analyses of the water samples were carried out at the Trace Analysis Laboratory, Faculty of Chemistry and Pharmacy, University of Sofia “St Kliment Ohridski” using ICP-MS Apparatus (Perkin-Elmer SCIEX Elan DRC-e) with a cross-flow nebulizer, following the analytical techniques of Lyubomirova *et al*. (2020a, b). The spectrometer was optimized (RF, gas flow, lens voltage) to provide minimal values of the ratios of oxides and double charged ions and maximum intensity of the analytes. The concentrations of 69 elements were

determined during the analyses, including REE and Y. Working standard solutions were prepared from ICP-MS multi-element calibration standard solution-2 (Ultra Scientific) and ICP-MS Multielement Standard B (High Purity Standards) with initial concentrations of 10 mg/L, to which single element standards of some elements (Fluka) with initial concentrations of 1000 mg/l were added after appropriate dilution (details in Lyubomirova *et al*., 2020a). External calibration by multi-element standard solution was performed. The calibration coefficients for all calibration curves were at least 0.99. The ICP-MS conditions for measurement of the elements of interest are given in Lyubomirova *et al*. (2020a, b). The simultaneous determination of all elements in the samples was achieved by reducing the signal of the macroelements thanks to the application of a Dynamic Bandpass Tuning parameter RPa (the DC potential between the pole pairs of the quadrupole cell that enables the high-mass cut off) using cell-based-ICP-MS (Lyubomirova *et al.*, 2020a, b).

RESULTS

Pore water profiles

The ICP-MS results for the REY concentrations in the pore water samples show variation of ΣREY from 4.05 µg/l (25–30 cm depth, station 3607) to 106 µg/l (0–5 cm depth, station 3615). The REE content of the pore waters is at least one order of magnitude higher than the oceanic water value (average bottom seawater after Li and Schoonmaker, 2014) and shows an enrichment of the middle and heavy REE. The REE of the host sediments (Hikov *et al*., 2022) show values that are two orders of magnitude higher than the studied pore waters.

Among the set of REE, La, Lu, and Ce are chosen and followed in the depth profiles of station 3607 as they are known to behave differently from the other REE in the water column (see review in Byrne and Sholkovitz, 1996) and may have distinct distribution in pore water. The variation in the absolute values of La, Ce, Y, and Lu were also compared to the variation in Fe, Mn and Co absolute values (Fig. 2) for a further geochemical interpretation. Cerium and Y reveal a shallow subsurface maximum (0–5 cm) and smooth decrease in depth, whereas La and Lu show an enrichment at the deeper level. The comparison between the absolute values of the elements above described in the pore waters to their values in seawater show an overall enrichment in the pore waters.

REY patterns

All REY patterns are normalized to Post-Archean Australian Shale (PAAS), using data of McLennan (1989). The REY normalization to PAAS was chosen, because it is considered more relevant for samples collected in the Pacific Ocean, in line with Alibo and Nozaki (1999), than those compiled from the North American Shale Composite (NASC).

PAAS-normalized REY patterns (Fig. 3) show an enrichment of HREY and MREY over LREY. The lowest La_{SN}/Yb_{SN} ratio (0.04) is observed for station 3615 for the subsurface sample (0–5 cm depth), and the highest value (0.63) for station 3609-1 for the deepest (25–30 cm) sample (Table 1). For a comparison, the seawater La_{SN}/Yb_{SN} is 0.276.

Positive and negative anomalies in the PAAS-normalized patterns of Ce, Eu and Y are calculated and presented in Table 1.

In our samples, the negative Ce/Ce* values (Fig. 4) predominate and vary from 0.25 to 0.82.

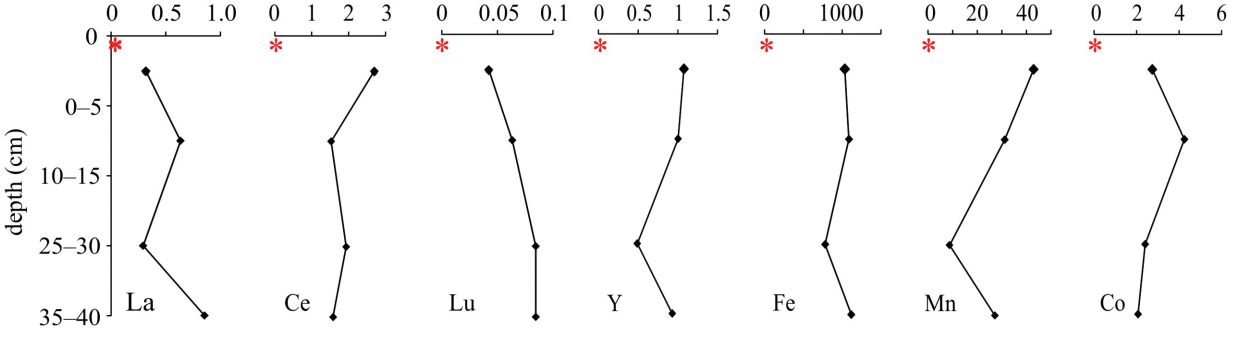

Fig. 2. Variation characteristics of La, Ce, Y, Lu, as well as the metals Fe, Mn and Co (in µg/l) in the pore water of station 3007 compared to their values in seawater (red asterisk).

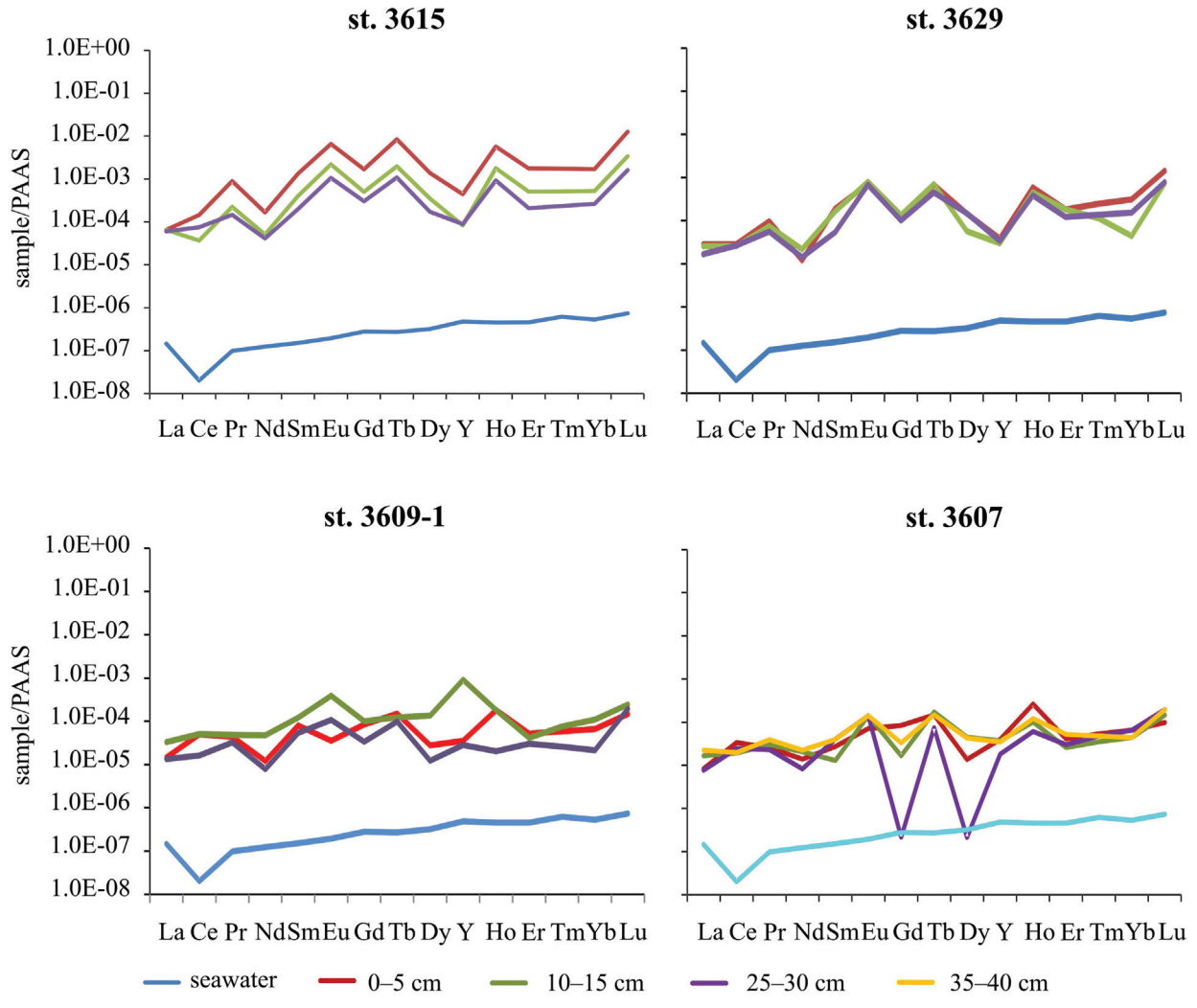

Fig. 3. PAAS-normalized REY patterns of the seawater and the pore water samples of stations 3615, 3629, 3609-1 and 3607.

Table 1
Cerium, europium and yttrium anomalies and La_{SN}/Yb_{SN} ratio of the pore waters of stations 3615, 3629, 3609-1 and 3607. $Ce/Ce^* = 2Ce_N/(La_N+Pr_N)$; $Eu/Eu^* = 2Eu_N/(Sm_N+Gd_N)$; $Y/Y^* = 2Y_N/(Dy_N+Ho_N)$; 1, 2, 3 and 4 correspond to the sampled layer depth, respectively 0–5, 10–15, 25–30 and 35–40 cm

	SeaW	3615			3629			3609-1			3607			
		1	2	3	1	2	3	1	2	3	1	2	3	4
Ce/Ce*	0.16	0.3	0.25	0.72	0.46	0.51	0.73	1.73	1.25	0.71	2.01	0.82	1.58	0.64
Eu/Eu*	0.9	4.31	4.87	4.24	4.92	5.29	8.80	0.43	3.53	2.44	1.28	9.63	6.99	3.87
Y/Y*	1.24	0.13	0.08	0.16	0.1	0.12	0.13	0.34	5.72	1.74	0.29	0.51	0.6	0.42
La_{SN}/Yb_{SN}	0.28	0.04	0.12	0.23	0.09	0.58	0.11	0.22	0.3	0.63	0.13	0.38	0.12	0.51

Positive values for Ce/Ce* are rarely found, *e.g.*, for station 3609-1 (1.73–1.25 for layer 1, 2), station 3607 (2.01 – layer 1, 1.58 – layer 3). The Ce/Ce* values increase with depth in two profiles (st. 3615, 3629), decrease in one profile (3609-1), and in one (st. 3607) do not exhibit any clear tendency.

The Eu/Eu* values vary between 0.43 (station 3609-1, layer 1) and 9.63 (station 3607, layer 2).

The highest Eu/Eu* values (up to 9.63) are found for the second layer samples in most of stations (3615, 3609-1, 3607). The Eu/Eu* values increase with depth for the samples from station 3629 and decrease in depth for the samples of station 3607 as it is illustrated on Fig. 4.

In the pore water sample set, the values for Y/Y* vary from 0.08 (station 3615, layer 2) to 5.72 (station 3609-1, layer 2). For stations 3609-1 and 3607, the highest are the Y/Y* values for the second layer, and for station 3615 the Y/Y* value is the lowest for the same layer. For stations 3615 and 3629, the values for Y/Y* increase with depth, as for stations 3609-1 and 3607 vary without any regularity.

DISCUSSION

The new data on the natural concentration for REY in the pore waters for four stations in the IOM exploration area make it possible to sort the distributions into groups that we believe are characteristic for the sedimentation and early diagenetic processes. Three types of REY distribution were outlined:

i) I type – elevated concentrations for REY for the layer 0–5 cm; the distribution is observed for stations 3615 and 3629. The concentrations for all REE and Y of layer 0–5 cm are distinctly higher than the other two layers. The distribution of the REE and Y concentrations among the layers for station 3629 is similar, but the concentration differences are small. Exceptions are Nd and Eu concentrations, as they are the highest for layer 10–15 cm;

ii) II type – elevated REY concentration predominantly for the layer 10–15 cm compared to the other layers; the distribution is characteristic for the pore waters of station 3609-1;

iii) III type – the REY elements show their maximal values in different layers, a distribution observed for the samples of station 3607.

Too few pore water points in depth profiles are available for the studied stations to make well-constrained statements about the REY concentration trend with depth. The natural variations in the absolute concentrations followed in the depth profiles for station 3607 (Fig. 2) show a shallow subsurface maximum at a depth 0–5 cm and a smooth decrease in depth for Ce and Y. The clear deeper sink in the REE concentration found for the pore water profiles from and the Western Pacific (see Deng *et al*., 2017, fig. 2) and the California margin sites (Haley *et al*., 2004) was not observed in the present study. Lanthanum and Lu show a tendency of enrichment in the deeper layers (Fig. 2). The small scale heterogeneity in REY distribution and the lack of a clear deeper sink found in the pore water profiles by Haley *et al*. (2004) and Deng *et al*. (2017) could be assigned to the small scale solid phase heterogeneity in the deep sea sediments described by Milakovska *et al*. (in preparation) for the IOM license area. Generally, there is an agreement the heterogeneity of deep-sea sediments to be a result of the burrowing activities of various organisms (Berger, 1967). Some of the

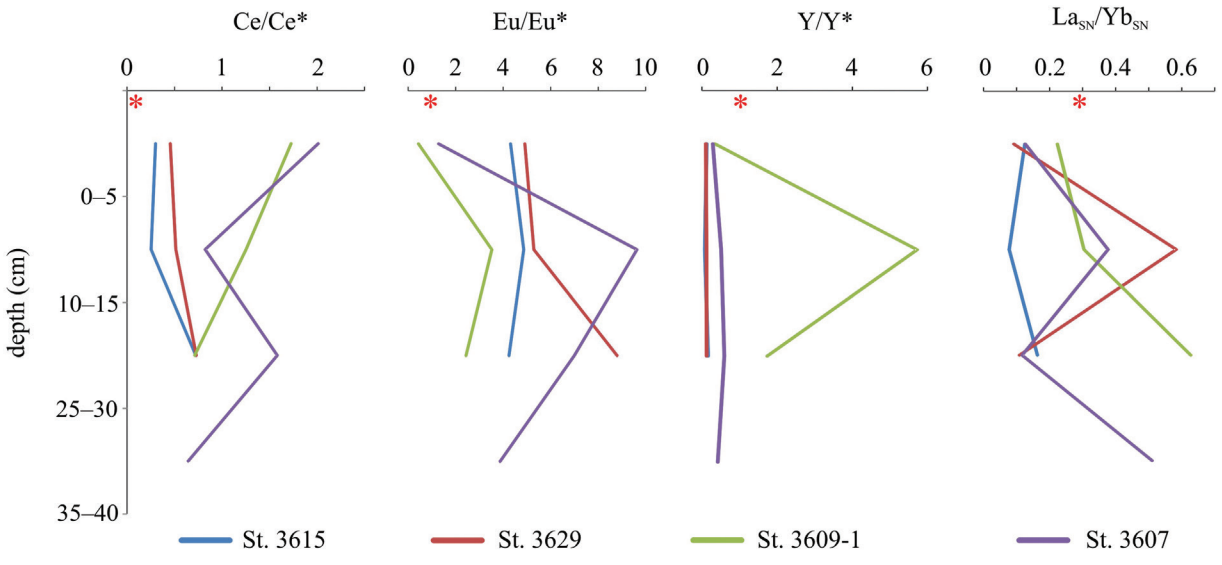

Fig. 4. Ce/Ce*, Eu/Eu*, Y/Y* and La_{SN}/Yb_{SN} patterns of distribution of the samples of stations 3615, 3629, 3609-1, and 3607 compared to the seawater (marked by a red asterisk).

vertical disturbance of pore water profiles (*e.g*., reported by Callender and Bowser, 1980) could also be interpreted as a result of burrowing activities of organisms. Consequently, some scatter in our REY data can be speculated upon that bioturbation has affected the sediment profiles.

The PAAS-normalized REY patterns of pore waters in marine sediments were summarized and grouped into the three types of patterns by Haley *et al*. (2004): "Linear", "HREE enriched" and "MREE bulge". The "Linear" and the "MREE bulge" are more typical for the cores with dissolved Fe. Our samples have REY values elevated over the seawater in a linear fashion from Ce to Lu, with predominantly negligible Ce-anomaly and negligible to distinct "MREE bulge". Similar are the REE patterns for pore water from the Western Pacific (Deng *et al*., 2017), Northern Cascadia accretionary margin (Kim *et al*., 2012) and California margin (Haley *et al*., 2004). These "type of patterns" serve to elucidate the processes that control the REEs in pore waters, broadly applicable for fingerprinting early diagenetic processes. The "linear" pattern is the most common type, describing a constant, but moderate increase in the PAAS-normalized REEs. This pattern type represents REEs released from the degradation of organic matter, as concluded by Haley *et al*. (2004). It is coupled with the increasing tendency of the REEs to complex with dissolved organic carbon (DOC) produced during the degradation process (Byrne and Sholkovitz, 1996).

The "MREE bulge" pattern is far more conspicuous than the other pattern types. The coincidence of pore water showing this pattern with the zone of greatest production of dissolved Fe strongly suggests according to Haley *et al*. (2004) that dissolution of a surficial, REE-enriched solid Fe-phase is the source of these REEs.

Another REY source for the pore waters is the hydrothermal input in addition to the DOC and dissolved Fe. The hydrothermal input represents a large, but likely secondary flux of REY to the ocean, and carries a flat or HREE depleted REY signal with excess europium concentrations (Bau and Dulski, 1996; Douville *et al*., 1999). Rivers are a major source of REY, and carry a flat "continental type" shale-normalized distribution pattern. The typical seawater REE profile (Fig. 3) is smooth and coherent with progressive enrichments in heavier REE and a distinct Ce/Ce* anomaly.

Our results show that REE concentrations exhibit a large dynamic range, and that REE fractionations reflect remineralization of organic coatings and the reduction of Fe and Ce oxides. We obtained relatively "flat" REE patterns with an almost complete absence of Ce anomaly that are typical of shallow open ocean REE patterns (Byrne and Sholkovitz, 1996).

The cerium anomaly (Ce/Ce*) is thought to be indicative of redox state (Elderfield, 1988; Byrne and Sholkovitz, 1996) because Ce has redox potential in the pH range of seawater. Anomalous concentrations of redox-sensitive Ce compared with neighboring REE originate in oxic water column conditions, and as such, Ce anomalies can provide a potentially useful redox proxy. Usually, negative (<1) Ce anomalies are typical of well-oxygenated seawater while positive (>1) Ce anomalies are expected under reducing conditions where soluble Ce^{3+} is more stable. The predominance of the negative values for the Ce anomaly in our samples indicates oxygenated seawater for most of the samples. The exceptions are some of the samples of stations 3609-1 and 3607, whose positive Ce anomaly indicates reducing pore water.

The studied pore waters show Eu anomaly (Eu/Eu*) values that are in the same range as reported for seawater by Tostevin *et al*. (2016). According to the positive values of Eu anomaly, the pore water samples are in most of the cases alkaline – between 0.43 (layer 1, st. 3609-1) and 9.63 (layer 2, st. 3607), in line with MacRae *et al*. (1992). Based on Eu^{3+}/Eu^{2+} equilibria in aqueous solution, MacRae *et al*. (1992) predict that Eu^{2+} should be highly stable at neutral to alkaline pH in strongly anoxic conditions, thus resulting in enhanced Eu abundances relative to Sm and Gd (*i.e.*, Eu/Eu*> 1). Such positive Eu anomalies have been reported also in hydrothermal systems associated with a Ca enrichment (*e.g*., Klinkhammer *et al*., 1994; Douville *et al*., 1999), but very little is known about the europium fractionation in highly reducing environment of the continental margin sediments, such as those associated with sulfidic and methanogenic zones. However, the Eu anomaly is not pronounced enough to interpret a clear signal.

The understanding of Y anomaly (Y/Y*) is somewhat limited, as many earlier studies did not include Y measurements alongside REEs. Larger Y anomalies (40–80) are described by Bau *et al*. (1997) and Nozaki and Zhang (1995) occurring in open-marine settings, and smaller (33–40) ones in near-shore or restricted settings. Our data are not in line with Bau *et al*. (1997) and Nozaki and Zhang (1995), as they are much lower than the values for both seawater and open-marine settings.

The bottom sediments, pore waters and polymetallic nodules form the real environment for the nodules formation. This environment is a result, according to Kotlinski and Stoyanova (2012) and

Hein *et al*. (2013), of sedimentation rate, bioturbation, oxidation conditions, certain bottom current conditions, and diagenetic process (biogeochemistry, adsorption, desorption, transformation and migration). The concentration of metals in the pore water depends on the accumulation rate of sediments and the processes of dissolution, reduction and oxidation, while in sediments and nodules the metal deposition depends on the presence of nucleus (fragments of old nodules, sediment material, volcanoclastic rocks, bioclastic material), well oxygenated bottom waters, semi-liquid surface layer and bioturbation (Kotlinski and Stoyanova, 2012). The nodules precipitate in two main types of environment: (i) hydrogenetic (from seawater), and (ii) diagenetic (from pore fluids). A third, mixed (hydrogenetic-diagenetic) type of environment is often reported (Hein *et al*., 2013).

The highest Eh values and elevated contents of Mn, Co, Cu, Ba and P are documented for sediments of station 3615 (Milakovska *et al*., 2021). The same station shows the highest REY contents of both sediments and pore waters that suggest some input from the neighboring volcanoes (Hikov *et al*., 2022). Elevated phosphorous content may also play an important role for the REE accumulation (Ren *et al*., 2021) for this station.

CONCLUSIONS

Our results indicate that the pore waters in the stations are predominantly in an oxidizing state of the environment. Ce and Y are slightly enriched around the water-sediment interface, *i.e.*, in the shallow sediment layer, while La and Lu are enriched in the deeper layers of sediments. PAAS-normalized REY of the pore waters display similar patterns, typically characterized by a pronounced negative Ce anomaly together with a little MREE enrichment. We assume that the decomposition of and adsorption on organic matter and oxidation conditions are the main factors for the fractionation of REE in pore water. The reason for some scatter in our REY data might most likely be linked to bioturbation that has affected the sediment profiles.

Acknowledgements

The authors are greatly indebted to the reviewers Prof. Irina Karadjova (Sofia University) and Dr. Petyo Filipov (Geological Institute, Bulgarian Academy of Sciences) for their critical remarks and suggestions. The study was partly supported by the Bulgarian National Science Fund grant KP-06-N34/6.

REFERENCES

Abbott, A., Löhr, S., Trethewy, M. 2019. Are Clay Minerals the Primary Control on the Oceanic Rare Earth Element Budget?. *Frontiers in Marine Science* 6, https://doi.org/10.3389/fmars.2019.00504.

Alibo, D.S., Nozaki, Y. 1999. Rare earth elements in seawater: particle association, shale-normalization, and Ce oxidation. *Geochimica et Cosmochimica Acta* 63 (3/4), 363–372, https://doi.org/10.1016/S0016-7037(98)00279-8.

Baláž, P. 2021. Results of the first phase of the deep-sea polymetallic nodules geological survey in the Interoceanmetal Joint Organization licence area (2001–2016). *Mineralia Slovaca* 53, 3–36.

Bau, M., Dulski, P., 1996. Distribution of yttrium and rare earth elements in the Penge and Kuruman iron-formations, Transvaal Supergroup, South Africa. *Precambrian Research* 79 (1–2), 37–55, https://doi.org/10.1016/0301-9268(95)00087-9.

Bau, M., Möller, P., Dulski, P., 1997. Yttrium and lanthanides in eastern Mediterranean seawater and their fractionation during redox-cycling. *Marine Chemistry* 56 (1–2), 123–131, http://dx.doi.org/10.1016/S0304-4203(96)00091-6.

Bowen, V.T., Noshkin, V.E., Livingston, H.D., Volchok, H.L. 1980. Fallout radionucleotides in the Pacific Ocean: vertical and horizontal distributions, largely from GEOSECS stations. *Earth and Planetary Science Letters* 49 (2), 411–434, https://doi.org/10.1016/0012-821X(80)90083-7.

Byrne, R.H., Kim, K.-H. 1990. Rare earth element scavenging in seawater. *Geochimica et Cosmochimica Acta* 54 (10), 2645–2656, https://doi.org/10.1016/0016-7037(90)90002-3.

Byrne, R.H., Sholkovitz, E.R. 1996. Marine chemistry and geochemistry of the lanthanides. *In:* Gschneider Jr., K.A., Eyring, L. (Eds), *Handbook on the Physics and Chemistry of Rare Earths Vol. 23*. Elsevier, Amsterdam, 497–592, https://doi.org/10.1016/S0168-1273(96)23009-0.

Callender, E., Bowser, C.J. 1980. Manganese and copper geochemistry of interstitial fluids from nodule-rich pelagic sediments of the northeastern equatorial Pacific Ocean. *American Journal of Science* 280, 1063–1096, https://doi.org/10.2475/ajs.280.10.1063.

Deng, Y., Ren, J., Guo, Q., Cao, J., Wang, H., Liu, C. 2017, Rare earth element geochemistry characteristics of seawater and porewater from deep sea in western Pacific. *Nature, Scientific Reports* 7, 16539, https://doi.org/10.1038/s41598-017-16379-1.

Douville, E., Bienvenu, P., Charlou, J.L., Donval, J., Fouquet, Y., Appriou, P., Gamo, T. 1999. Yttrium and rare earth elements in fluids from various deep-sea hydrothermal systems. *Geochimica et Cosmochimica Acta* 63 (5), 627–643.

Elderfield, H. 1988. The Oceanic Chemistry of the Rare Earth Elements. *Philosophical Transactions of the Royal Society A* 325, 105–126, https://doi.org/10.1098/rsta.1988.0046.

Elderfield, H., Greaves, M.J. 1982. The rare earth elements in seawater. *Nature* 296, 214–219, https://doi.org/10.1038/296214a0.

Haley, B., Klinkhammer, G., McManus, J. 2004. Rare earth elements in pore waters of marine sediments. *Geochimica et Cosmochimica Acta* 68 (6), 1265–1279, https://doi.org/10.1016/j.gca.2003.09.012.

Hein, J., Mitzell, K., Koschinsky, A., Conrad, T. 2013. Deep-ocean mineral deposits as a source of critical metals for high- and green-technology applications: Comparison with land-based resources. *Ore Geology Reviews* 51, 1–14, https://doi.org/10.1016/j.oregeorev.2012.12.001.

Hikov, A., Milakovska, Z., Stoyanova, V., Stefanova, E., Abramowski, T., Chavdarova, S., Stavrev, M. 2022. REE and trace elements distribution in the deep-sea sediments from the Interoceanmetal (IOM) polymetallic nodule exploration area in the Clarion-Clipperton fractures zone, NE Pacific. *Comptes rendus de l'Académie bulgare des Sciences* 75 (7), 1018–1027, https://doi.org/10.7546/CRABS.2022.07.10.

Homoky, W., Weber, T., Berelson, W., Conway, T., Henderson G., van Hulten, M., Jeandel, C., Severmann, S., Tagliabue, A., 2016. Quantifying trace element and isotope fluxes at the ocean–sediment boundary: a review. *Philosophical Transactions of the Royal Society* A 374 (2081), https://doi.org/10.1098/rsta.2016.0246.

ISBA/19/LTC/8. 2013. *Recommendations for the guidance of contractors for the assessment of the possible environmental impacts arising from exploration for marine minerals in the Area*. International Seabed Authority, Issued by the Legal and Technical Commission 13-24713, 32 pp., https://www.isa.org.jm/documents/isba19ltc8.

Jarvis, I. 1985. Geochemistry and origin of Eocene-Oligocene metalliferous sediments from the central equatorial Pacific. *In:* Mayer, L.A., Theyer, F., Barron, J.A., Dunn, D.A., Handyside, T. (Eds), *Initial Reports of the Deep Sea Drilling Project* 85, 781–804, doi:10.2973/dsdp.proc.85.1985.

Kashiwabara, T., Toda, R., Nakamura, K., Yasukawa, K., Fujinaga, K., Kubo, S., Nozaki, T., Takahashi, Y., Suzuki K., Kato, Y. 2018. Synchrotron X-ray spectroscopic perspective on the formation mechanism of REY-rich muds in the Pacific Ocean. *Geochimica et Cosmochimica Acta* 240, 274–292, https://doi.org/10.1016/j.gca.2018.08.013.

Kato, Y., Fujinaga, K., Nakamura, K., Takaya, Y., Kitamura, K., Ohta, J., Toda, R., Nakashima, T., Iwamori, H. 2011. Deep-sea mud in the Pacific Ocean as a potential resource for rare-earth elements. *Nature Geoscience* 4, 535–539, https://doi.org/10.1038/ngeo1185.

Kim, J.-H., Torres, M., Haley, B., Kastner, M., Pohlman, J., Riedel, M., Lee, Y.-J., 2012. The effect of diagenesis and fluid migration on rare earth element distribution in pore fluids of the northern Cascadia accretionary margin. *Chemical Geology* 291, 152–165, https://doi.org/10.1016/j.chemgeo.2011.10.010.

Klinkhammer, G., Elderfield, H., Edmond, J.M., Mitra, A. 1994. Geochemical implications of rare earth element patterns in hydrothermal fluids from mid-ocean ridges. *Geochimica et Cosmochimica Acta* 58 (23), 5105–5113, https://doi.org/10.1016/0016-7037(94)90297-6.

Kotlinski, R, Stoyanova, V. 2012. *Nodule coverage, morphology and distribution in the Eastern CCZ*. ISA, Technical Study No 6: Prospector's Guide for Polymetallic Nodule Deposits in the Clarion-Clipperton Fracture Zone, 34–42.

Li, Y.-H., Schoonmaker, J.E. 2014. Chemical Composition and Mineralogy of Marine Sediments. *Treatise on Geochemistry* 9 (1), 1–35, https://doi.org/10.1016/B0-08-043751-6/07088-2.

Livingston, H.D., Anderson R.F. 1983. Large particle transport of plutonium and other fallout radionucleotides to the deep ocean. *Nature* 303, 228–231, https://doi.org/10.1038/303228a0.

Lyubomirova, V., Mihaylova, V., Djingova, R. 2020a. Chemical characterization of Bulgarian bottled mineral waters. *Journal of Food Composition and Analysis* 93, 103595, https://doi.org/10.1016/j.jfca.2020.103595.

Lyubomirova, V., Mihaylova, V., Djingova, R. 2020b. Determination of macroelements in potable waters with cell-based inductively-coupled plasma mass spectrometry. *Spectroscopy Europe* 32 (5), 18–21.

MacRae, N.D., Nesbitt, H.W., Kronberg, B.I. 1992. Development of a positive Eu anomaly during diagenesis. *Earth and Planetary Science Letters* 109 (3–4), 585–591, https://doi.org/10.1016/0012-821X(92)90116-D.

McLennan, S. 1989. Rare earth elements in sedimentary rocks: influence of provenance and sedimentary processes. *In:* Lipin, B.R., McKay, G.A. (Eds), *Geochemistry and Mineralogy of Rare Earth Elements*. De Gruyter, Berlin, 169–200, https://doi.org/10.1515/9781501509032-010.

Milakovska, Z., Stoyanova, V., Hikov, A., Abramowski, T., Stefanova, E., Peytcheva, I., Chavdarova, S., Stavrev, M. 2021. Depositional setting of the deep-sea sediments from an area of high nodule occurrence in the Clarion-Clipperton Fractures Zone, NE Pacific. *Goldschmidt 2021 Abstracts*, https://doi.org/10.7185/gold2021.5983.

Milakovska, Z., Stoyanova, V., Hikov, A., Abramowski, T., Stefanova, E., Peytcheva, I. (in preparation). Local variability in the sedimentary environment in an area of high nodule occurrence in the Clarion-Clipperton Fracture Zone, NE Pacific.

Nozaki, Y., Zhang, J. 1995. The rare earth elements and yttrium in the coastal/offshore mixing zone of Tokyo Bay waters and the Kuroshio. *In:* Sakai, H., Nozaki, Y. (Eds), *Biogeochemical Processes and Ocean Flux in the Western Pacific*. Terra Scientific Publishing Company (TERRAPUB), Tokyo, 171–184.

Paul, S., Volz, J., Bau, M., Köster, M., Kasten, S., Koschinsky, A. 2019. Calcium phosphate control of REY patterns of siliceous-ooze-rich deep-sea sediments from the central equatorial Pacific. *Geochimica et Cosmochimica Acta* 251, 56–72, https://doi.org/10.1016/j.gca.2019.02.019.

Ren, J., Liu, Y., Wang, F., He, G., Deng, X., Wei, Z., Yao, H. 2021. Mechanism and influencing factors of REY enrichment in deep-sea sediments. *Minerals* 11 (2) 196, 1–16, https://doi.org/10.3390/min11020196.

Skowronek, A, Maciag, L., Zawadzki, D., Strzelecka, A., Baláž, P., Mianowicz, Abramowski, T., Konečný, P., Krawcewicz, A. 2021. Chemostratigraphic and textural indicators of nucleation and growth of polymetallic nodules from the Clarion-Clipperton Fracture Zone (IOM Claim Area). *Minerals* 11 (8) 868, 1–38, https://doi.org/10.3390/min11080868.

Tostevin, R., Shields, G., Tarbuck, G., He, T., Clarkson, M., Wood, R. 2016. Effective use of cerium anomalies as a redox proxy in carbonate-dominated marine settings. *Chemical Geology* 438, 146–162, https://doi.org/10.1016/j.chemgeo.2016.06.027.

Zhang, L., Algeo, T., Cao, L., Zhao, L., Chen, Z., Li, Z. 2016. Diagenetic uptake of rare earth elements by conodont apatite. *Palaeogeography, Palaeoclimatology, Palaeoecology* 458, 176–197, https://doi.org/10.1016/j.palaeo.2015.10.049.

Zhang, J., Nozaki, Y. 1996. Rare earth elements and yttrium in seawater: ICP-MS determinations in the East Caroline, Coral Sea, and South Fiji basins of the western South Pacific Ocean. *Geochimica et Cosmochimica Acta* 60 (23), 4631–4644, https://doi.org/10.1016/S0016-7037(96)00276-1.